Toxicology and Applied Pharmacology 279 (2014) 53–62

Contents lists available at ScienceDirect

Toxicology and Applied Pharmacology

journal homepage: www.elsevier.com/locate/ytaap

A novel dihydropyridine with 3-aryl *meta*-hydroxyl substitution blocks L-type calcium channels in rat cardiomyocytes

David Galvis-Pareja [a,b], Gerald Zapata-Torres [c], Jorge Hidalgo [b,d], Pedro Ayala [b], Zully Pedrozo [a,b,d], Cristián Ibarra [b,e,f], Guillermo Diaz-Araya [f], Andrew R. Hall [g], Jose Miguel Vicencio [a,g], Luis Nuñez-Vergara [h,1], Sergio Lavandero [a,b,d,i,*]

[a] Advanced Center for Chronic Diseases (ACCDiS), Facultad de Ciencias Químicas y Farmacéuticas & Facultad Medicina, Universidad de Chile, Santiago, Chile
[b] Centro Estudios Moleculares de la Célula (CEMC), Facultad de Ciencias Químicas y Farmacéuticas & Facultad Medicina, Universidad de Chile, Santiago, Chile
[c] Departamento de Química Inorgánica y Analítica, Facultad de Ciencias Químicas y Farmacéuticas, Universidad de Chile, Santiago, Chile
[d] Instituto de Ciencias Biomédicas, Facultad de Medicina, Universidad de Chile, Santiago, Chile
[e] Department of Medical Biochemistry and Biophysics, Karolinska Institutet, 17177 Stockholm, Sweden
[f] Cardiovascular and Metabolic Diseases iMed, AstraZeneca R&D, 43183 Mölndal, Sweden
[g] The Hatter Cardiovascular Institute, University College London, London, UK
[h] Departamento de Química Farmacológica y Toxicológica, Facultad de Ciencias Químicas y Farmacéuticas, Universidad de Chile, Santiago, Chile
[i] Department of Internal Medicine/Cardiology Division, University of Texas Southwestern Medical Center, Dallas, TX, USA

ARTICLE INFO

Article history:
Received 10 January 2014
Revised 13 April 2014
Accepted 9 May 2014
Available online 17 May 2014

Keywords:
Calcium
Dihydropyridine
Heart
Cardiomyocytes
L-type calcium channels

ABSTRACT

Rationale: Dihydropyridines are widely used for the treatment of several cardiac diseases due to their blocking activity on L-type Ca^{2+} channels and their renowned antioxidant properties.
Methods: We synthesized six novel dihydropyridine molecules and performed docking studies on the binding site of the L-type Ca^{2+} channel. We used biochemical techniques on isolated adult rat cardiomyocytes to assess the efficacy of these molecules on their Ca^{2+} channel-blocking activity and antioxidant properties. The Ca^{2+} channel-blocking activity was evaluated by confocal microscopy on fluo-3AM loaded cardiomyocytes, as well as using patch clamp experiments. Antioxidant properties were evaluated by flow cytometry using the ROS sensitive dye 1,2,3 DHR.
Results: Our docking studies show that a novel compound with 3-OH substitution inserts into the active binding site of the L-type Ca^{2+} channel previously described for nitrendipine. In biochemical assays, the novel *meta*-OH group in the aryl in C4 showed a high blocking effect on L-type Ca^{2+} channel as opposed to *para*-substituted compounds. In the tests we performed, none of the molecules showed antioxidant properties.
Conclusions: Only substitutions in C2, C3 and C5 of the aryl ring render dihydropyridine compounds with the capacity of blocking LTCC. Based on our docking studies, we postulate that the antioxidant activity requires a larger group than the *meta*-OH substitution in C2, C3 or C5 of the dihydropyridine ring.

Introduction

Voltage-dependent calcium (Ca^{2+}) channels (VDCC) are widely expressed throughout different tissues and importantly in the cardiovascular system, where they represent the main route for cellular Ca^{2+} entry that couples electrical excitation to contraction. These channels are multimeric proteins that consist of a principal α_1 subunit forming the permeation pore, which associates with the auxiliary subunits $\alpha_2\delta$, β and γ. Among the different types of VDCC, predominantly the L-type calcium channel (LTCC) is found in cardiomyocytes, where it is a key component of the contractile cycle (Ertel et al., 2000). Due to the relevance of the LTCC in cardiac diseases, this channel is the primary target of several pharmacological agents. There are different families of LTCC inhibitors; dihydropyridines such as nifedipine and nitrendipine are the most widely used, followed by phenylalkylamines such as verapamil, or benzothiazepines like diltiazem (Colecraft et al., 2002). The amino acid sequence of the α_1 subunit is organized in four repeated domains (I to IV). Each one of them contains six transmembrane segments (S1 to S6), a membrane-associated loop between S5 and S6, as well as both N- and C-termini facing the intracellular side. In each domain, S4 constitutes the voltage sensor. Domains III and IV contain the specific binding sites for all Ca^{2+} channel blockers

* Corresponding author at: Advanced Center for Chronic Diseases (ACCDiS), Facultad de Ciencias Químicas y Farmacéuticas, Universidad de Chile, Olivos 1007, Santiago 8380492, Chile. Fax: +56 2 2978 2912.
E-mail address: slavander@uchile.cl (S. Lavandero).
[1] Deceased.

http://dx.doi.org/10.1016/j.taap.2014.05.004
0041-008X/

found so far; these are located in III S5, III S6, and IV S6 for dihydropyridines, and III S6 and IV S6 for the other members of the Ca^{2+} channel blocker family (Ertel et al., 2000; Walsh et al., 2009). The 1,4-dihydropyridines (DHPs) are the most important of these therapeutic agents (Krzeminski et al., 2011; Triggle, 2007). By binding to and blocking the α_{1C} subunit, they display a negative inotropic effect, which is characterized by a decrease in the force of contraction of the myocardium (Schramm et al., 1983). They also slow down the conduction of electrical activity during the plateau phase of the action potential of the heart, resulting in a negative chronotropic effect that lowers the heart rate (Millard et al., 1983). This negative chronotropic effect of Ca^{2+} channel blockers (CCBs) makes them useful drugs for patients with atrial fibrillation or flutter. Additionally, the resulting lower heart rates represent lower cardiac oxygen requirements and promote better adaptability to adrenergic tone (Scholz, 1997).

The relevance of reactive oxygen species (ROS) in cardiovascular disease has been well established. They are an aggravating and accelerating factor in the progress of cardiac pathologies. Changes in the cellular redox environment can affect the gating properties of ion channels, and because cardiac contraction is highly dependent on the regulation of intracellular Ca^{2+} levels ($[Ca^{2+}]_i$), redox modification of Ca^{2+} channels and transporters has a profound effect on cardiac function (Kourie, 1998). Key components of the cardiac excitation–contraction (EC) coupling machinery such as the sarco–endoplasmic reticulum Ca^{2+} ATPase (SERCA) and LTCC are subject to redox modulation, which is directly involved in cardiac pathologies. Significant bursts of reactive oxygen species (ROS) generation occur during reperfusion of the ischemic heart, and changes in the activity of the major components of $[Ca^{2+}]_i$ regulation, such as ryanodine receptors, Na^+–Ca^{2+} exchangers and Ca^{2+} ATPases, are likely to play an important role in ischemia-related Ca^{2+} overload (Kourie, 1997; Waring, 2005).

In this regard, dihydropyridines have been the subject of intensive research over the last four decades. Their discovered antioxidant activity gave birth to very versatile molecules, which are classified as third generation DHPs with strong LTCC blocking effects and also with attributed antioxidant properties. We have been investigating new DHPs that could combine both properties. In our studies we synthesized six differently substituted DHP molecules, we studied their LTCC blocking activity and their antioxidant properties and found that only a novel 3-OH substituted DHP displayed a strong LTCC blocking activity but did not exhibit antioxidant effects as well as the rest of these newly synthesized DHPs.

Materials and methods

Isolation and culture of adult rat cardiomyocytes. Adult rats were bred in the Animal Breeding Facility from the Facultad de Ciencias Químicas y Farmacéuticas, Universidad de Chile (Santiago, Chile). We performed all studies with the approval of the institutional bioethical committee from Facultad de Ciencias Químicas y Farmacéuticas, Universidad de Chile, Santiago. This investigation conforms to the "Guide for the Care and Use of Laboratory Animals" published by the United States National Institutes of Health. Adult rat ventricular myocytes (ARVMs) were prepared from the hearts of male Sprague Dawley rats (2–3 months, 250–300 g). Animals were anesthetized by an intraperitoneal (i.p.) injection of ketamine:xilazine 2:1. The heart was removed via thoracotomy and transferred to a Gerard ice-cold solution. The aorta was cannulated and the heart mounted into a Langendorff apparatus then successively perfused with the following oxygenated solutions: Gerard buffer (Ca^{2+} 2.6 mM), to allow recovery of spontaneous activity; nominally Ca^{2+}-free Gerard buffer supplemented with EGTA (2.5 mM) until contraction ceased and then digestion solution supplemented with collagenase type A and 2,3-butanedione monoxime (BDM), for 30 min. Once flaccid, the heart was rinsed for 2 min without collagenase. Ventricles were removed and finely minced and gently triturated, then placed in 15 mL of digestion solution, at 37 °C under constant and soft agitation for 10 min; after which the supernatant was transferred to a Falcon tube and centrifuged at 500 rpm for 2 min. The pellet was gently resuspended in a Gerard buffer supplemented with BDM. For microscopy and patch clamp experiments, ARVMs were then seeded in coverslips precoated with laminin (5 μg/mL). After 20–30 min the buffer was changed and replaced with M199/HEPES/Ca^{2+} 2 mM, supplemented with penicillin–streptomycin. Further BDM supplementation was used only for patch clamp experiments. ARVMs were used on the same day of isolation (Communal et al., 1998; Snabaitis et al., 2005). Neonatal rat ventricular cardiomyocytes (NRVM) were prepared as previously established (Foncea et al., 1997). Briefly, NRVM were isolated from the hearts from one- to three-day-old Sprague Dawley rats by enzymatic digestion. Cells were pre-plated to discard non-myocyte cells. NRVM were maintained in DMEM:M199 (4:1) medium with 10% (w/v) FBS and penicillin–streptomycin before experiments. NRVM were either used in suspension, shortly (2 h) after isolation for ROS measurements and analysis by flow cytometry, or were plated on gelatin-precoated dishes and treated according to different experimental conditions; cells were then trypsinized and used in suspension for flow cytometry analyses to measure cell viability.

Dynamic Ca^{2+} measurements. Dynamic Ca^{2+} measurements were performed on an inverted confocal microscope (Carl Zeiss Axiovert 200 Pascal5-LSM Microsystems). Experiments were performed on the same day as the cardiomyocytes were isolated. Cardiac myocytes were washed three times with Ca^{2+}-containing resting media (Krebs buffer (mM): 145 NaCl, 5 KCl, 2.6 $CaCl_2$, 1 $MgCl_2$, 10 HEPES-Na, 5.6 glucose, pH 7.4), to remove M199 culture medium, and loaded with 5.4 μM Fluo 3-AM (coming from a stock in 20% pluronic acid, DMSO) for 30 min at room temperature. After loading, ventricular myocytes were washed with the same buffer and used immediately thereafter (Pravdic et al., 2009). The cell-containing coverslips were mounted in a 1 mL capacity plastic chamber and placed in the confocal microscope for fluorescence measurements after excitation with a 488-nm wavelength argon laser beam or filter system. Fluorescence measurements were performed on individual cardiomyocytes. Line-scan images were acquired at a sampling rate of 15.8 msec per line, along the longitudinal axis of the cell, avoiding crossing the nucleus. An objective lens Plan Apo 63X (numerical aperture 1.4) and a pinhole of 1 Airy unit disk were used. In all acquisitions, the image dimension was 512 × 120 pixels. Intracellular Ca^{2+} was expressed as a percentage of fluorescence intensity. All line scan images of Ca^{2+} transients were background subtracted (Pearl et al., 2011). Compounds were added after 30 s of initiating the recordings. The action peak was defined at 240 s. We used linescan analysis for the assessment of chronotropy, by quantifying the frequency of fluorescence spots obtained from the linescan pictures and inotropy from the fluorescence intensity.

ROS measurements. All tests were performed on a FACSCanto flow cytometer (BD Biosciences) with a 2-laser configuration, 488/633 nm. To study the antioxidant capacity of our different DHPs, we used the fluorescent dye dihydrorhodamine 1 2 3 (DHR 1,2,3) at 25 μM, a probe to study various species of ROS. Flow cytometry allows the analysis of cells in suspension, but the particle size ranges from 0.2 to 50 μm. Large cells such as ARVM (>100 μm) cannot be analyzed by flow cytometry, therefore we used NRVM, as they provide the closest validated model for cardiac cell-based studies. To measure ROS levels we used a previously described protocol (Mashimo and Ohno, 2006). Briefly, neonatal rat cardiomyocytes suspended at a density of 3×10^5/mL with either Krebs-Ringer (mM: 145 NaCl, 5 KCl, 2.6 $CaCl_2$, 1 $MgCl_2$, 10 HEPES-Na, 5.6 glucose, pH 7.4) or Krebs-Ringer plus the compounds. After 30 min of incubation, the cells were centrifuged again and the supernatant medium replaced with Krebs-Ringer containing the ROS producing stimulus H_2O_2 (100 μM) for 1 h. After this, the probe DHR

1,2,3 was added for 30 min and the samples were then washed and analyzed by flow cytometry.

Cell viability. NRVM were plated in gelatin-coated plates after isolation. After 24 h, they were incubated for 24 h with different DHPs or with H_2O_2 as a positive control to trigger cell death, negative control cells were treated with the vehicle DMSO (0.1% v/v). Non-adherent cells were collected and adherent cells were trypsinized. Both adherent (live) and non-adherent (dead or dying) cells were pooled and stained with the vital dye propidium iodide to label dead cells. Fluorescence of dead cells was analyzed using a FACSCanto flow cytometer (BD Biosciences).

LTCC homology model. We used for this study a previously built homology model of the LTCC, kindly provided by Dr. Zhorov (Tikhonov and Zhorov, 2008). This model contains transmembrane segments S5 and S6 and P-loops from the four repeats. All segments far from the DHP binding site were not included in the model. Among available X-ray structures that could serve as templates for modeling different states of $Ca_v1.2$, Zhorov et al. used KvAP for the open state, which is a voltage-dependent K^+ channel from *Aeropyrum pernix* (Jiang et al., 2003), based on the voltage-gating properties shared by both channels. The closed state of $Ca_v1.2$ was modeled using KcsA, a closed K^+ channel template structure (Jiang et al., 2003). The selectivity filter region was built using the $Na_v1.4$ P-loop domain model as a template (a voltage-gated Na^+ channel, which belongs to the superfamily of P-loop channels, which includes K^+ and Ca^{2+} channels) (Tikhonov and Zhorov, 2005). We designated residues using labels, which are universal for P-loop channels. A residue label includes the domain (repeat) number (1 to 4), segment type (p, P-loop; i, the inner helix; o, the outer helix), and relative number of the residue in the segment. The energy expression included van der Waals, electrostatic, H-bonding, hydration, and torsion components, as well as the energy of deformation of bond angles in DHPs. The bond angles of the protein were kept rigid and the hydration energy was calculated by the implicit solvent method. Non-bonded interactions were calculated using the software AMBER force field version 12 (Case et al., 2012), which is consistent with the implicit solvent approach. The energy was minimized in the space of generalized coordinates, which include all torsion angles, bond angles of the ligand, positions of ions, and positions and orientations of root atoms of ligands. The channel models and their complexes with ligands were optimized by the Monte Carlo minimization (MCM) method. To ensure similar backbone geometry with the X-ray template, C^{α} atoms of the model were pinned. The proposed specific interactions between ligands and DHP-sensing residues were imposed by distance constraints. Thus, DHP-LTCC H-bonds were imposed with distance constraints that allow penalty-free separation of the H-bonding atoms up to 2.2 Å. The complexes MC minimized with the distance constraints were refined in unconstrained MCM trajectories to ensure that the proposed models are energetically stable. All calculations were performed with the ZMM program (Tikhonov and Zhorov, 2009).

Docking analysis. Molecular docking of DHPs at the LTCC homology model was investigated using the Lamarckian genetic algorithm search method as implemented in Morris et al. (1998) The receptor was kept rigid, while full flexibility was allowed for the ligands to translate/rotate. Polar hydrogens were added to the receptors and Kollman-united atom partial charges along with atomic solvation parameters were assigned to the individual protein atoms. Previous to docking studies, the three-dimensional structures of each ligand were generated and then energy minimized using Gaussian98 software. Rigid root and rotatable bonds were assigned automatically using AutoDock tools (Morris et al., 1998), polar hydrogens were removed and the partial charges from these were added to the carbon (Gasteiger charges). The atom type for aromatic carbons was reassigned in order to use the AutoDock 4.0 aromatic carbon grid map. Docking was carried out using $60 \times 60 \times 60$ grid points with a default spacing of 0.375 Å. The grid was positioned to include the full ligand-binding site in the central part of the α_1 subunit so as to allow extensive sampling around residue Y 216. Within this grid, the Lamarckian genetic search algorithm was used with a population size of 150 individuals, calculated using 200 different runs (i.e. 200 dockings). Each run had two stop criteria, a maximum of 1.5×10^6 energy evaluations or a maximum of 50,000 generations, starting from a random position and conformation; default parameters were used for the Lamarckian genetic algorithm search (Tikhonov and Zhorov, 2008, 2009).

Patch clamp. Single cell voltage clamp recordings were obtained from isolated adult rat cardiomyocytes, with an Axopatch 1D patch clamp amplifier under the whole-cell modality. Holding potential was set at −80 mV. Glass micropipettes (G85150T-3 Warner Instruments) with a tip resistance in the range of 1 to 3 M Ω were obtained with a pipette puller and fire polished with a microforge. Once a seal was formed between the pipette tip and the cell membrane, the whole-cell patch configuration was obtained by gentle suction applied to the inside of the pipette. The rupture of the section of membrane sealed against the tip was monitored by a 2 mV test pulse and verified by the increase in the transient capacitive current trace. The membrane capacity was obtained from the integration of the current transient obtained for a −10 mV pulse. The pipette (intracellular) ionic composition was (mM): Cs-methanesulfonate 150, EGTA 5, $MgCl_2$ 5, Hepes 10 adjusted to pH 7.3 with CsOH. The external saline composition was TEA-Cl 140, $MgCl_2$ 2, $CaCl_2$ 1.5, glucose 10 and HEPES 10. For the voltage clamp stimulus protocol, the pClamp suite of programs was used. Clampex 5.5 was used to generate the command voltage protocol as family of 16 pulses of 50 ms duration and stepped from 10 mV above the holding potential (usually −80 mV) with an 8 mV increment between them. In this manner, the protocol voltage range covered from −70 to +58 mV. The net current at each voltage step was obtained after the cancelation of the linear components of the capacity and conductance by subtraction of 6 pulses of the inverse polarity and 1/6 of the amplitude (P/6 protocol). For data acquisition, the family of the net current signals for a protocol run was filtered at 5 KHz and digitized at 15 KHz. Data generated was stored for off-line analysis. For analysis of membrane current from voltage clamp recordings, the net inward current obtained during the pulse protocol was considered to be carried mostly by Ca^{2+} ions due to ionic composition of the extra and intracellular solutions. With the Clampfit program, the peak magnitude of this current was tabulated to generate I–V curves after being normalized for membrane capacity (nA/nF). The value of the peak current obtained at 20 mV showed throughout the records to be the largest. Because each cell studied has control and test values, all the data can be normalized and grouped. The grouped data was adjusted to a single site dose–response curve.

Reagents and treatments. EDTA, EGTA, butane 2,3 monoxime (BDM), M199 medium, Dulbecco's modified Eagle's medium (DMEM); dihydrorhodamine 1,2,3 (DHR 1,2,3), as well as basic grade biochemical reagents were obtained from Sigma Chemical Co (St. Louis, MO, USA). Fetal bovine serum (FBS), fetal calf serum (FCS), penicillin and streptomycin were acquired from Biological industries. Laminin and Fluo3-acetoxymethyl ester (Fluo3-AM) were purchased from Invitrogen. The synthesis of the DHP compounds used in this study, as well as the purity analyses conducted have been described previously (Nunez-Vergara et al., 2007; Salazar et al., 2008). These new DHP molecules were named according to the substituent(s) in the aryl ring in C4.

Statistical analysis. Results are presented as mean ± SEM. Treatment was analyzed by one-way ANOVA with post-hoc examination by Bonferroni test, and it was considered statistically significant if $P < 0.05$. For the frequency chart a Student's t-test was performed.

Statistical evaluation was carried out using Graph Pad Prism 5 (GraphPad Software, San Diego, Calif., USA).

Results

Para-substitutions on the aryl ring in C4 keep DHPs out of the LTCC binding pocket

We synthesized six new DHP molecules based on the structure of the DHP nitrendipine (NIT, Fig. 1a), replacing the *meta*-substituent NO_2 in the bowsprit zone of the molecule for different groups as well as introducing new *para*-substitutions on the aryl ring (Nunez-Vergara et al., 2007; Salazar et al., 2008). This resulted in 6 new DHP molecules: C4(4-phenyl)-1,4-dihydropyridine (PDHP, Fig. 1b), C4(3-hydroxyphenyl)-1,4-dihydropyridine (3-OH, Fig. 1c), C4(3,5-dihydroxyphenyl)-1,4-dihydropyridine (3,5-OH, Fig. 1d), C4(4-hydroxyphenyl)-1,4-dihydropyridine (4-OH, Fig. 1e), C4(4-vanillin)-1,4-dihydropyridine (VDHP, Fig. 1f), C4(4-isovanillin)-1,4-dihydropyridine (IDHP, Fig. 1g). In our first approach, we checked theoretically if all our new compounds enter inside the binding pocket of a previously built LTCC model, kindly provided by Dr. Zhorov (Tikhonov and Zhorov, 2009). The model was validated by using nimodipine, which docked itself in the same spot where DHP previously docked on this model, and for which the interactions were already described (Tikhonov and Zhorov, 2009). NIT was the molecule docked as control (Fig. 2a), and we observed that its interactions were the same as those described for nimodipine. For the new DHPs, our findings showed that only three of our novel molecules bound to critical amino acid residues of the binding pocket, namely 3,5-OH, 3-OH and PDHP (Figs. 2b–d), and these DHPs were those lacking the *para*-substitution in the aryl ring in C4. The only DHP that interacted with the channel in the same way as NIT was 3,5-OH (Fig. 2b), prompting us to expect a similar inhibitory effect in cell culture based experiments. In the case of 3-OH (Fig. 2c), the presence of a hydroxyl group in the aryl ring opposite to the critical M4i12 residue suggests that an interaction can happen, specifically as this hydroxyl group could freely rotate; however, the distance between the oxygen atom of the hydroxyl group and the sulfur atom of the methionine residue at M4i12 would be too far (7.07 Å), making an interaction unlikely or too weak. In the case

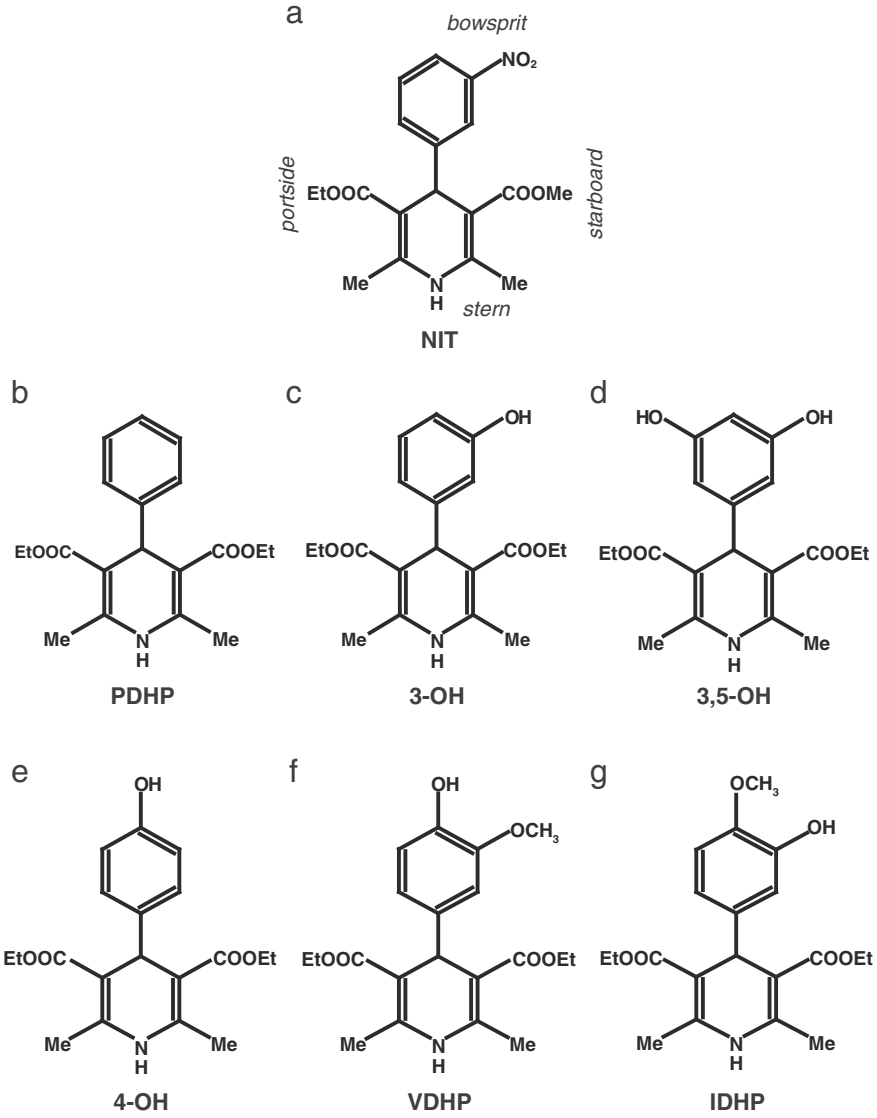

Fig. 1. Structure of 6 novel DHP molecules tested in this study. a) Nitrendipine (NIT) was used as control throughout the study. b) C4(4-phenyl)-1,4-dihydropyridine (PDHP). c) C4(3-hydroxyphenyl)-1,4-dihydropyridine (3-OH). d) C4(3,5-dihydroxyphenyl)-1,4-dihydropyridine (3,5-OH). e) C4(4-hydroxyphenyl)-1,4-dihydropyridine (4-OH). f) C4(4-vanillin)-1,4-dihydropyridine (VDHP). g) C4(4-isovanillin)-1,4-dihydropyridine (IDHP).

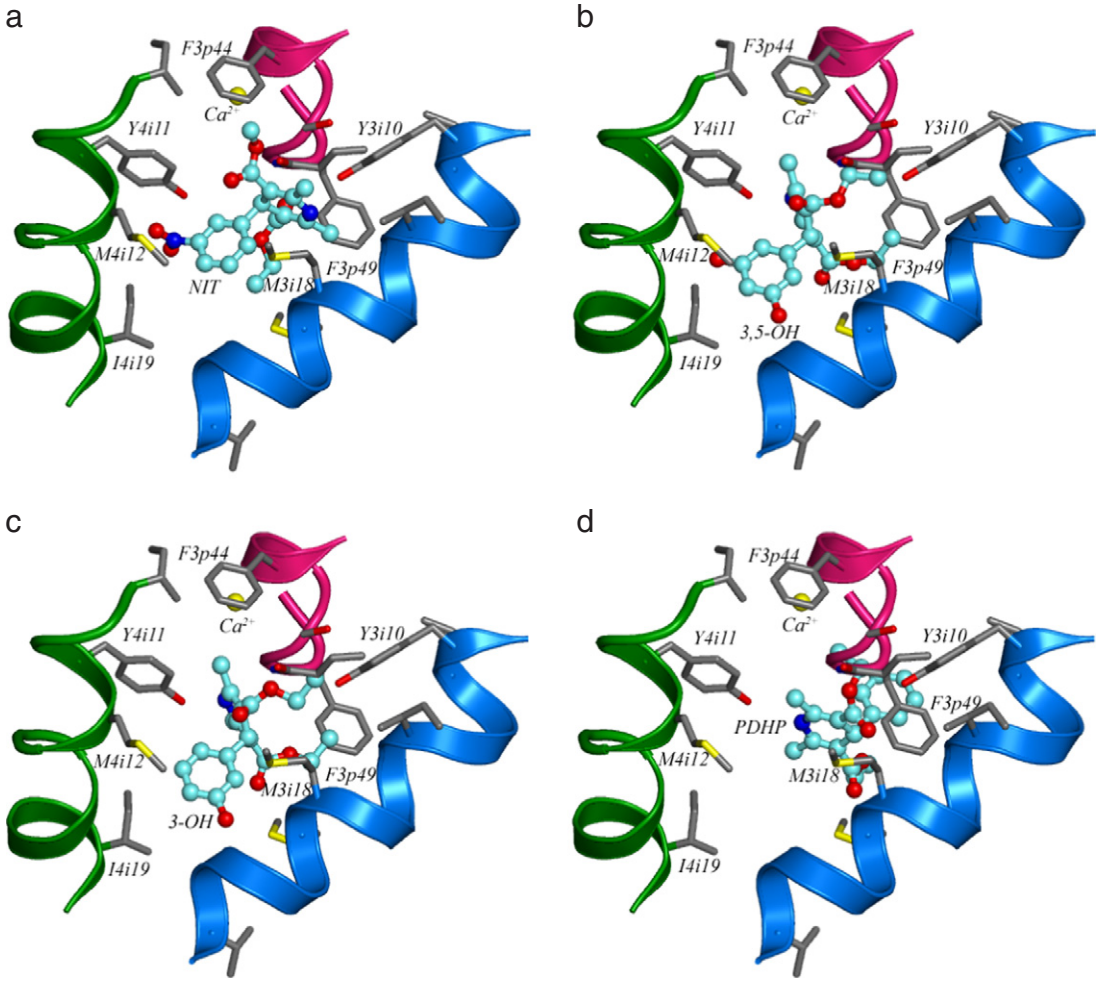

Fig. 2. Orientation of NIT and new DHP molecules in the homology model of LTCC. S6, P, and S5 helices are shown, respectively, as by smooth ribbons, sharp ribbons, and strands. Repeat III is green, repeat IV is purple, and repeats I and II are cyan. Ca^{2+} ions are shown as yellow spheres. DHP-sensing residues are shown by thin sticks and ligands are shown by thick sticks. a) Cytoplasmic view of the model with NIT, the bowsprit interacts with M4i12. b) Cytoplasmic view of the model with 3,5-OH, similar interaction was observed with M4i12. c) Cytoplasmic view of the model with 3-OH, no direct interaction but a close disposition between the aryl ring and the M4i12 residue is observed. d) Cytoplasmic view of the model with PDHP, no interaction with M4i12 was observed. For all molecules, the portside group does not approach the Ca^{2+} ion chelated by the selectivity filter glutamates in repeats III and IV.

of PDHP (Fig. 2d), the unsubstituted aryl ring indicates that any possible interactions between the substituents and amino acid residues would be missing, diminishing its theoretical effect on blocking the channels. Therefore, we could expect a Ca^{2+} antagonist effect in cell culture experiments for these three molecules. Regarding the new *para*-substituted DHPs and their inability to get inside the binding pocket of LTCC, we propose that this might be due to a sterical hindrance, so we set out to test them all in cell culture using adult rat cardiomyocytes, to further corroborate what we had just seen in our docking studies.

Effects of new DHPs on inotropy and chronotropy

We subjected primary adult rat cardiac myocytes to dynamic Ca^{2+} measurements using confocal microscopy in line scan mode. We evaluated two parameters in all compounds, inotropy and chronotropy. Inotropy was assessed as the ability of the compounds to inhibit Ca^{2+} transients, which correlates to a reduction in the fluorescence intensity of spontaneous Ca^{2+} activity. We first validated that vehicle itself had no effect (Supplementary Fig. 1) and that our positive control (NIT) exhibited inhibitory properties on fluorescence intensity. We tested three different concentrations of NIT, 0.1, 1 and 10 μM. The lowest concentration tested exhibited a significant reduction on fluorescence intensity after 120 and 180 s (Fig. 3a). We continued to test the same concentrations in our different compounds, but only 3-OH behaved similarly to NIT, exhibiting significant inhibitory properties after 180 s at a low concentration (Fig. 3b). The rest of the compounds failed to show any significant inhibitory properties (Fig. 3c and Supplementary Fig. 2).

We then tested the chronotropy inhibitory properties of the compounds using the above-mentioned three concentrations. Chronotropy was assessed as their ability to reduce the frequency of spontaneous Ca^{2+} activity. Similarly to the observed effects on inotropy, only 3-OH exhibited a significant reduction in the frequency of spontaneous Ca^{2+} oscillations, at comparable levels to NIT (Figs. 4a and b). The molecules 3,5-OH and PHDP showed no inhibitory properties (Figs. 4c and d). The molecules 4-OH, VDHP or IDHP showed no properties on chronotropy (Supplementary Fig. 3).

Based on the previous results, we performed patch clamp experiments to test the effect of 3-OH, the one compound that antagonized the channel in confocal microscopy experiments, compared to the control, NIT. The rates of conductance decrease between 3-OH and NIT exhibited similar shapes, and their IC50 values were similarly found in the nM range (Fig. 5a). 3-OH showed to be a very consistent trigger of current inhibition at different concentrations in the nM range (Fig. 5b). These whole-cell patch clamp experiments clearly confirmed our fluorescence microscopy experiments, indicating that the novel 3-

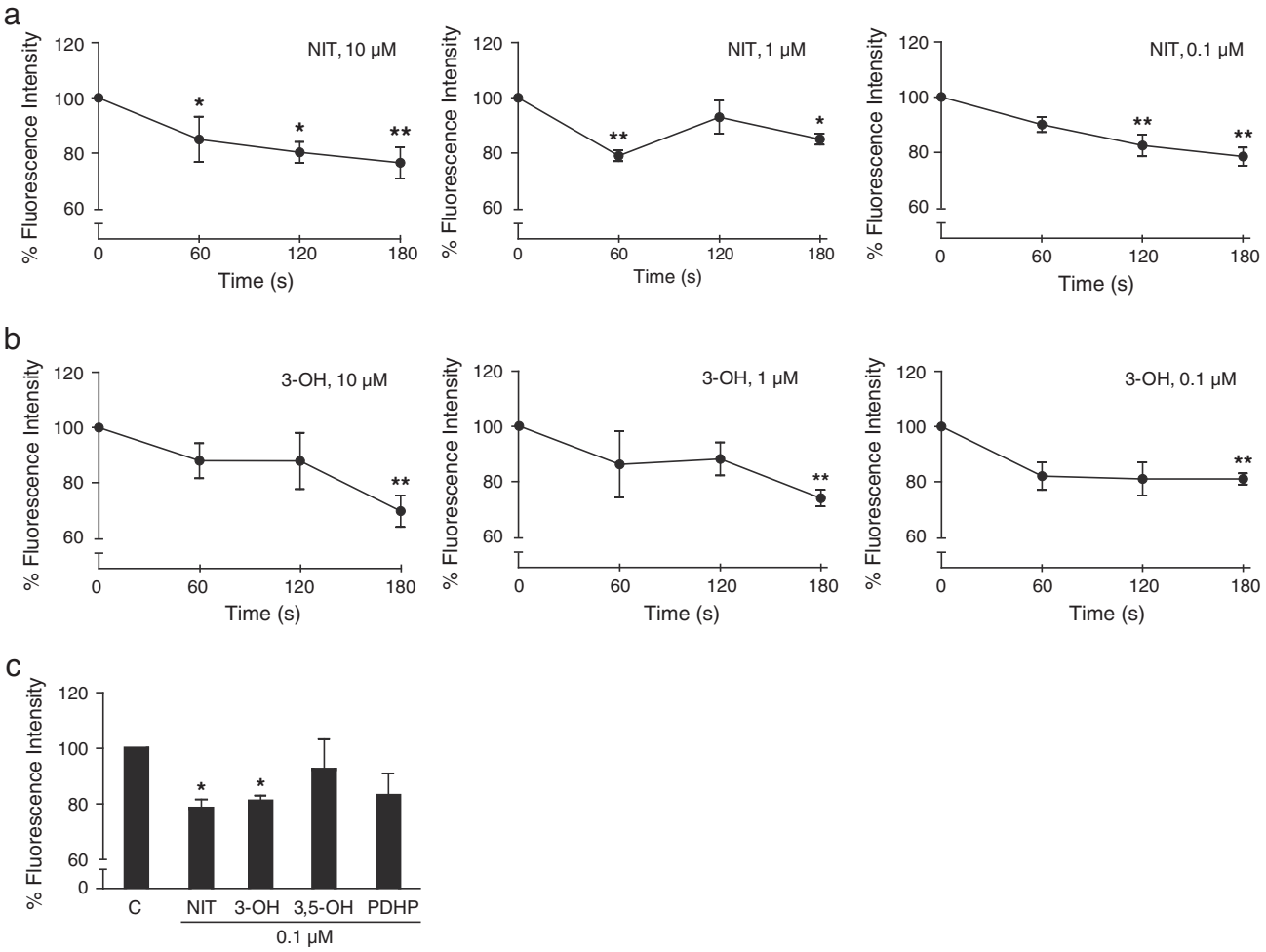

Fig. 3. Effect of novel DHP molecules on basal calcium oscillations in isolated adult rat ventricular myocytes. Quantification of global cytosolic Ca^{2+} levels by fluorescence intensity from fluo-3 loaded adult rat cardiac myocytes using confocal microscopy. a) Normalized values of fluorescence intensity to baseline, in the presence of different concentrations of NIT as indicated, studied dynamically at different times. b) Normalized values of fluorescence intensity to baseline, in the presence of different concentrations of 3-OH as indicated, studied dynamically at different times. c) Summary of all molecules at 180 s used at a concentration of 0.1 μM. Data are expressed as mean ± SEM, n = 3–5. *P < 0.5 and **P < 0.05 vs. control.

OH is a potent blocker of LTCC. This type of substitution characterized by a hydroxyl in *meta*-position of the aryl ring has never been described before in the literature, representing a novel type of DHP molecule with strong calcium channel antagonist properties.

The effects of new DHPs on ROS levels and viability

We subsequently tested these compounds and their antioxidant capacity in cultured neonatal cardiomyocytes by flow cytometry using the redox-sensitive dye DHR 1,2,3. We started by measuring baseline ROS levels in the absence or presence of the ROS scavenger N-acetylcysteine (NAC). The addition of H_2O_2 to the cell suspension increased ROS levels and NAC significantly reduced the elevation in ROS induced by peroxide (Fig. 6a). Using this setting we moved to study the effect of each one of the novel DHP compounds on ROS production. There were no differences in the amount of ROS detected at baseline with or without the addition of NAC or any of the Ca^{2+} antagonist compounds except for IDHP. In the presence of H_2O_2, IDHP significantly reduced the amount of ROS (Figs. 6a and h). However, these results were not replicated by any of the other Ca^{2+} antagonists, with no effect observed for 3,5-OH, 3-OH, 4-OH, VDHP, or the control drug NIT (Figs. 6b, d, e, f and g) in the presence of H_2O_2. In fact, and contrarily to what we expected, the addition of PDHP actually increased the levels of ROS (Fig. 6c). These results do not replicate the previously reported chemical based assays in which DHPs showed antioxidant activity, with only one of the novel DHPs possessing the antioxidant activity expected. Altogether, our results clearly indicate that 3-OH substitution in the aryl ring renders DHP molecules with a strong Ca^{2+} channel blocking activity, without clear effects on ROS reduction. To determine if our new DHPs have toxicity effect we tested cell viability in NRVM through flow cytometry analysis of the incorporation of the vital dye propidium iodide. Only PDHP 10 μM showed a small but significant more cell death from the control (Fig. 7). These data suggest that our DHPs did not have cytotoxicity effects in the cardiomyocytes at lower concentration and only PDHP exhibits a low toxicity effects in the cardiomyocytes.

Discussion

The compounds tested and described here base their chemical structure upon the potent LTCC inhibitor NIT, with several chemical alterations made to study their Ca^{2+} antagonist properties, as well as their antioxidant properties. While the modeling of the compounds was encouraging with PDHP, 3-OH and 3.5-OH, where all modeled to bind to the LTCC, Ca^{2+} transient experiments followed by patch clamp studies revealed that only 3-OH was able to inhibit the LTCC. The inhibition observed with 3-OH was comparable to that observed with NIT, with similar IC50 values observed for both drugs (1.2×10^{-8} M for NIT and 2.9×10^{-7} M for 3-OH). The ability of these compounds to reduce the antioxidant stress induced by H_2O_2 was also tested. Only one of our compounds, IDHP mediated a significant reduction in ROS, despite not

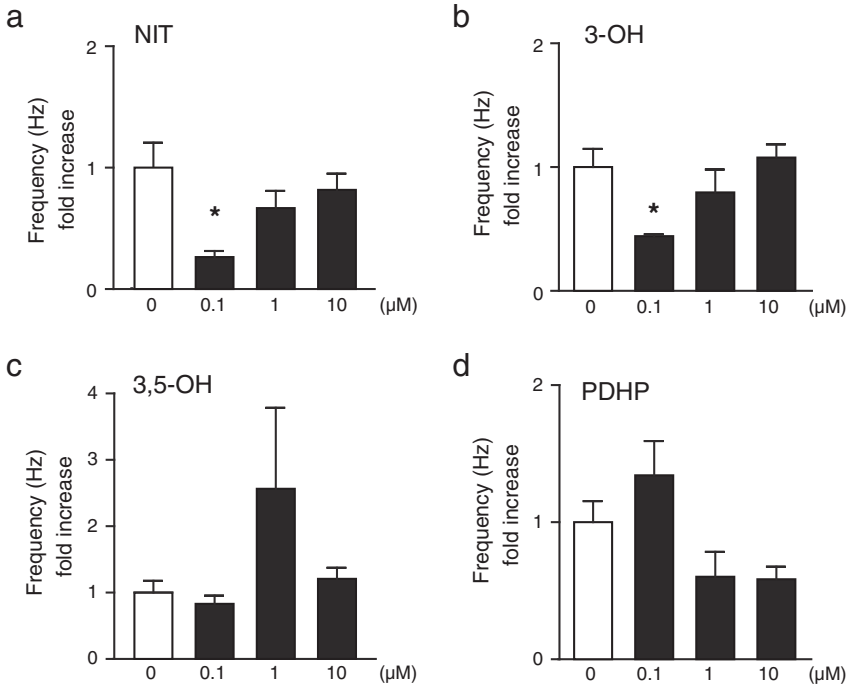

Fig. 4. Inhibition of spontaneous Ca^{2+} oscillations triggered by novel DHP molecules on adult cardiomyocytes. The reduction in spontaneous Ca^{2+} oscillations was measured by confocal microscopy in linescan mode using fluo-3 loaded primary adult rat cardiomyocytes. Data is shown as fold increase over the frequency (Hz) of oscillations under control conditions. Data are expressed as mean ± SEM, n = 3–5. *P < 0.5 vs. control (0 μM).

being a potent Ca^{2+} antagonist. In summary, none of the compounds tested here inhibited both the LTCC and provided protection against antioxidant stress.

Based on our LTCC inhibition studies, where we observed quite a disparity between the positive hits from the computing modeling and the cell based assays, we conclude that it is necessary to test the effects of modeled drugs in cell-based experiments. The docking studies utilized Zhorov's model of the LTCC, in which they modeled LTCC inhibition using the antagonist nimodipine (Tikhonov and Zhorov, 2009). Nimodipine is very similar to NIT with the only difference being a larger alkyl chain in C3. They reported a favorable stern-to-Y3i10 orientation of nimodipine in the LTCC pore and went on to verify the key DHP-sensing residues for nimodipine identified in previous mutational studies. In all docking models for the novel ligands described here, the LTCC was in a Ca^{2+} deficient state with the selectivity filter region loaded with a single Ca^{2+} ion. This configuration was selected because the Ca^{2+} deficient state is proposed to favor binding of DHP antagonists (Peterson and Catterall, 2006). The LTCC model for docking studies represents the molecule in an ideal state but does not account for alternative interactions of the ligand outside its binding site or the ability of the DHP to enter the binding pocket. An example of this, and possibly the biggest disparity between the modeling and cell-based experiments, was observed with 3,5-OH. 3,5-OH is predicted to fit into the binding site in exactly the same manner as NIT, proposing it to be a potent LTCC inhibitor. However, the compound had no effect in cell-based assays. The reason for this disparity could be the two polar hydroxyl substituents that 3,5-OH possesses. As such, the ability of 3,5-OH to form hydrogen bonds with other proteins is greatly increased, which may inhibit its ability to actually access into the LTCC. Concerning all *para*-substituted DHPs used in our studies: 4-OH, VDHP and IDHP, all

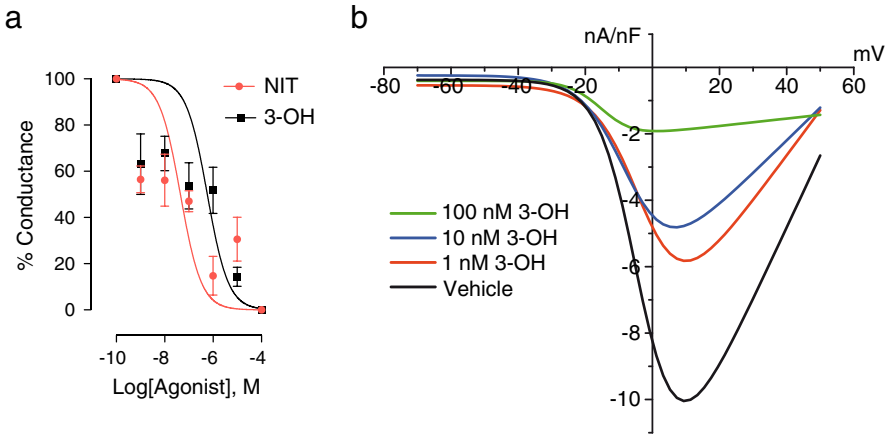

Fig. 5. Effect of NIT and 3-OH on patch clamp currents. Whole-cell patch clamp was performed on adult rat cardiomyocytes. a) Ratio of conductance decrease values for NIT and 3-OH respectively, using different mol/l concentrations. NIT, IC50 = 45×10^{-9} M. 3-OH, IC50 = 57×10^{-8} M. b) Average traces of current inhibition in whole cell experiments, using 3-OH at different concentrations as indicated. Data are representative of 3–5 independent experiments.

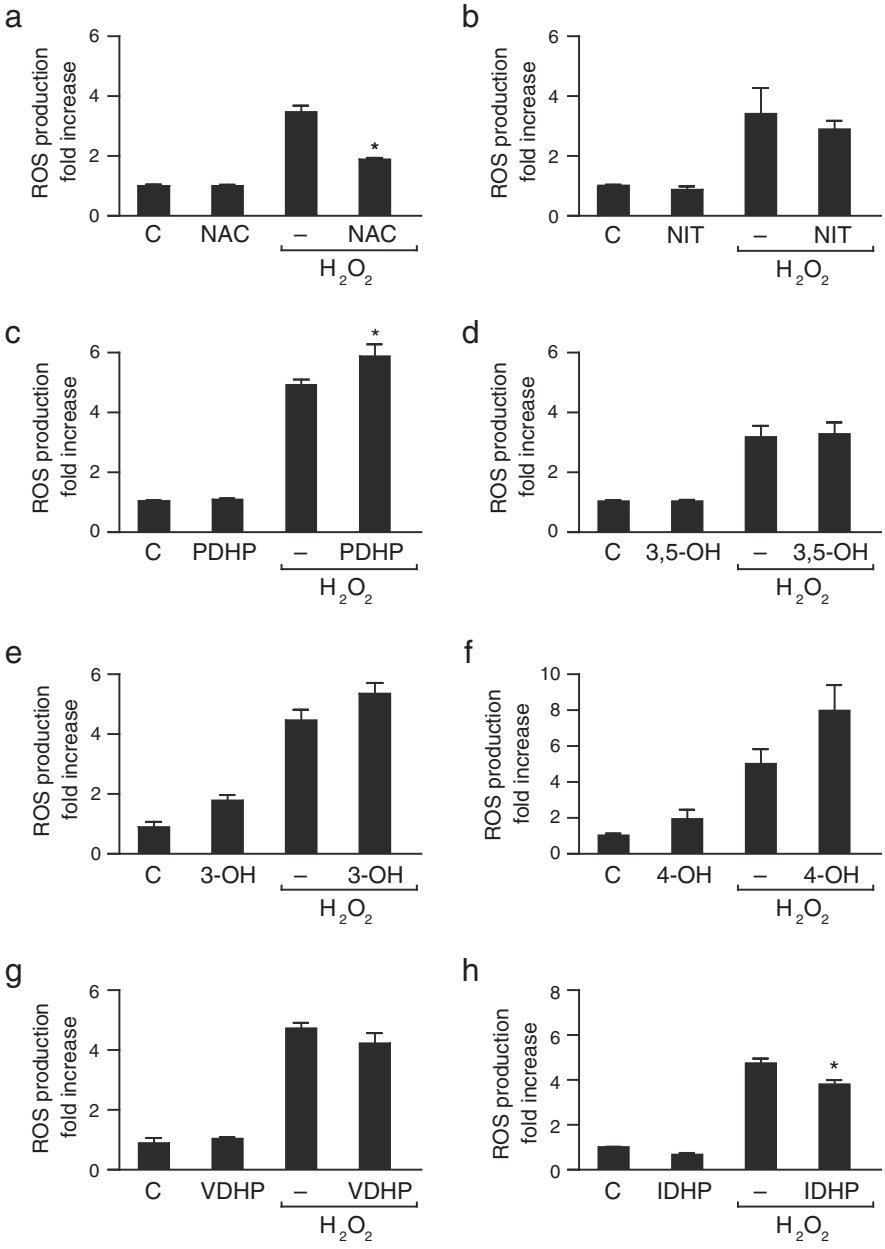

Fig. 6. Antioxidant activity of new DHPs. Neonatal rat cardiac myocytes were used for flow cytometry analyses in combination with the fluorescent ROS indicator dihydrorhodamine 1,2,3. N-acetylcysteine (NAC) was used as a positive antioxidant control and H_2O_2 was used to induce ROS accumulation. Fluorescence values were normalized to control and are expressed as mean ± SEM. All compounds were tested at a 10 μM. n = 3–5 Comparison among different treatment compounds was analyzed by one-way ANOVA with post-hoc examination by Bonferroni test. *P < 0.05 vs. control.

of them bound to the LTCC, but not in the binding pocket; confirming our hypothesis that a steric hindrance inhibits their ability to bind to the action site.

In 3-OH, as well as in NIT, the NH group at the stern forms an H-bond with Y3i10. The starboard methyl group fits into a hydrophobic pocket formed by I3i14 and M3i18. The portside group is bound in a hydrophobic pocket formed by M3i19, F3p49, and I4i19. For 3-OH, the polar OH group at the bowsprit accepts an H-bond from the side chain of Y4i11. The carbonyl oxygen at the starboard accepts an H-bond from Q3o18. The side chain of T3o14 does not interact with the DHP molecule directly, but it is exposed toward the starboard group in such a way that its enlargement would sterically prevent DHP binding, as showed by our docking results.

For, PDHP, the interactions were all the same but in the aryl ring in C4 it was different, as there was no substituting group, the interaction with Y3i10 is absent. The lack of this interaction might explain why PDHP did not block at 1 and 0.1 μM concentrations, as it would render its interaction with the binding site weak, thus inhibition only being observed at very high concentrations (10 μM).

Our experimental findings showed that only 3-OH inhibited the LTCC at all concentrations tested. When studying the chemical structures of the DHPs tested, 3-OH most closely resembles that of the DHP control, NIT—the main difference being the 3-OH substituent in the aryl rings in C4 at *meta* position. The nature of the substituent is different in each compound, for instance NIT bears a nitro group, which is an electron withdrawing substituent, whereas 3-OH having a hydroxyl group, is an electron releaser group. Both have the capacity to form hydrogen bonds, but as the literature states, the one with an electron withdrawing substitution would appear to be most effective in blocking LTCCs (Coburn et al., 1988; Triggle et al., 1980), which is absolutely in

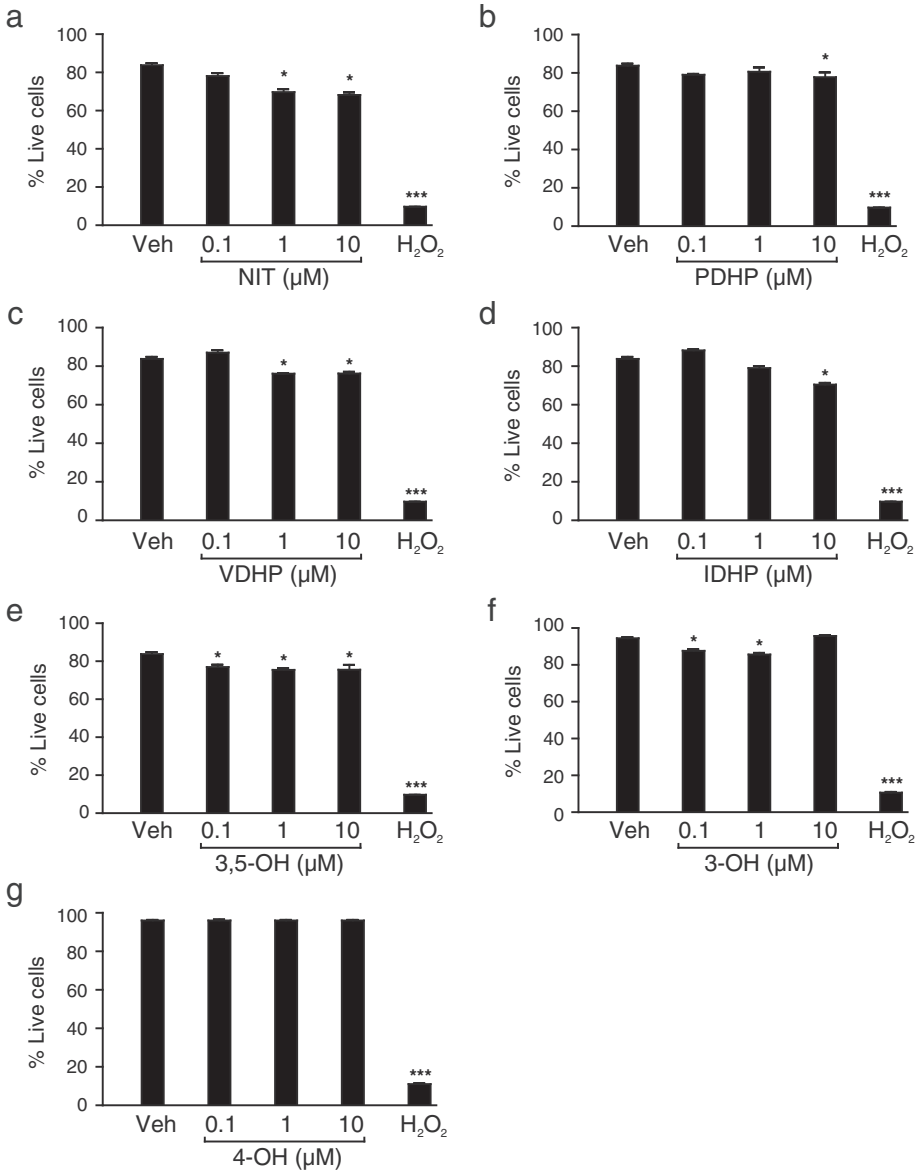

Fig. 7. Assessment of the toxicity of DHPs on neonatal rat cardiomyocytes. Cells were incubated for 24 h with different DHPs, or with H_2O_2 as a positive control to trigger cell death. Adherent and non-adherent cells were collected and stained with the vital dye propidium iodide to label dead cells. Fluorescence of dead cells was analyzed by flow cytometry. The percentage of live cells is shown as mean ± SEM. Comparison among different treatment compounds vs. control (vehicle) was analyzed by one-way ANOVA with post-hoc examination by Dunnett test. *$P < 0.1$ and ***$P < 0.01$ vs. control.

agreement with our results, where at all concentrations requires less time to start blocking the calcium channels.

There is increasing evidence indicating that the degree of free radical generation correlates with the progression of cardiovascular diseases. This has stimulated research for molecules that can conjugate several pharmacological activities (Nakamura et al., 2009). As it was described previously, our group has conducted extensive research in developing new DHP molecules with an antioxidant capacity. These drugs have been successfully tested in cell-free assays and in rat brain slices (Diaz-Araya et al., 1998; Lopez-Alarcon et al., 2003; Nunez-Vergara et al., 2003, 2007). Our present results show that only IDHP possesses any antioxidant effect. These results are inconsistent with those already published in molecule based assays. A possible explanation for this could be in the experimental approach using DHR 1,2,3, which may be insufficient to demonstrate the molecular antioxidant properties. For all DHP molecules, an antioxidant effect is expected in the plasma membrane, in close proximity to the LTCC. DHR 1,2,3 is a dye that distributes throughout the entire cell, and therefore may be indicating responses in locations or microdomains out of the target of interest. Regarding the chemical structure of the compounds, substituents in C4 of the DHP ring have been reported to be very effective antioxidants in compounds such as vanillin (Diaz-Araya et al., 1998; Nunez-Vergara et al., 2003, 2007). However, the molecules studied here lack a large substituent in C2 or C3 of the dihydropyridine ring which has been reported to be an absolute requirement for antioxidant properties in in-vitro assays (Mason et al., 1999b). Such large substituents are characteristic features of third generation DHPs, such as amlodipine or felodipine (Hishikawa and Luscher, 1998; Sugawara et al., 1996). The long substituent in C3 or C5 of the dihydropyridine ring allows these third generation compounds to easily penetrate the plasma membrane and interact with the LTCC while possessing additional antioxidant/pleiotropic actions. These highly lipophilic DHPs insert into the plasma membrane and are capable of donating protons to lipid peroxide molecules, thereby preventing lipid peroxidation (Bauerle and Seelig, 1991; Mason and Trumbore, 1996; Mason et al., 1999a). Therefore, to improve the antioxidant action of the novel DHPs tested here, the addition of a long

substituent in either C3 or C5 on dihydropyridine ring appears to be beneficial. Another possibility why we did not detect any antioxidant activity from our DHP compounds may be due to technical reasons, where we measured ROS with a protocol that uses cardiomyocytes in suspension for the treatments and for further analysis by flow cytometry. Our protocol used cardiac myocytes shortly after isolation to minimize the time between isolation and the stimulation of ROS, which can happen if cardiac myocytes are kept too long without cell adhesion, leading to cell death. A similar protocol has been used previously for measuring Ca^{2+} transients (Xu and Gopalakrishnan, 1991), without an impact on cell viability as it could be expected due to working with cardiomyocytes in suspension. In addition, we validated internally the efficacy of our protocol by using a positive control—NAC, which did decrease ROS levels as expected (Fig. 6).

In summary, we present here novel evidence in favor of a 3-OH *meta*-substitution in the aryl ring of DHP molecules, with a potent effect inhibiting LTCC. Further or more meticulous studies are necessary to ascertain the efficacy of this substitution on reducing ROS levels.

Conflict of interest

None declared.

Acknowledgments

We are grateful to Dr. B. Zhorov for kindly sharing his LTCC homology model. We dedicate this article to Dr. Luis Núñez-Vergara, whose sudden death was a great loss for us all. This work was supported by grant FONDAP 15130011 (SL), Anillo ACT 1111 (SL) and FONDECYT 1050761 (LNV).

Appendix A. Supplementary data

Supplementary data to this article can be found online at http://dx.doi.org/10.1016/j.taap.2014.05.004.

References

Bauerle, H.D., Seelig, J., 1991. Interaction of charged and uncharged calcium channel antagonists with phospholipid membranes. Binding equilibrium, binding enthalpy, and membrane location. Biochemistry 30, 7203–7211.

Case, D.A., Darden, T.A., Cheatham III, T.E., Simmerling, C.L., Wang, J., Duke, R.E., Luo, R., Walker, R.C., Zhang, W., Merz, K.M., Roberts, B., Hayik, S., Roitberg, A., Seabra, G., Swails, J., Goetz, A.W., Kolossváry, I., Wong, K.F., Paesani, F., Vanicek, J., Wolf, R.M., Liu, J., Wu, X., Brozell, S.R., Steinbrecher, T., Gohlke, H. Cai Q., Ye, X., Wang, J., Hsieh, M.-J., Cui, G., Roe, D.R., Mathews, D.H., Seetin, M.G., Salomon-Ferrer, R., Sagui, C., Babin, V., Luchko, T., Gusarov, S., Kovalenko, A., Kollman, P.A., 2012. AMBER 12. University of California, San Francisco.

Coburn, R.A., Wierzba, M., Suto, M.J., Solo, A.J., Triggle, A.M., Triggle, D.J., 1988. 1,4-Dihydropyridine antagonist activities at the calcium channel: a quantitative structure-activity relationship approach. J. Med. Chem. 31, 2103–2107.

Colecraft, H.M., Alseikhan, B., Takahashi, S.X., Chaudhuri, D., Mittman, S., Yegnasubramanian, V., Alvania, R.S., Johns, D.C., Marban, E., Yue, D.T., 2002. Novel functional properties of Ca^{2+} channel beta subunits revealed by their expression in adult rat heart cells. J. Physiol. 541, 435–452.

Communal, C., Singh, K., Pimentel, D.R., Colucci, W.S., 1998. Norepinephrine stimulates apoptosis in adult rat ventricular myocytes by activation of the beta-adrenergic pathway. Circulation 98, 1329–1334.

Diaz-Araya, G., Godoy, L., Naranjo, L., Squella, J.A., Letelier, M.E., Nunez-Vergara, L.J., 1998. Antioxidant effects of 1,4-dihydropyridine and nitroso aryl derivatives on the Fe^{+3}/ascorbate-stimulated lipid peroxidation in rat brain slices. Gen. Pharmacol. 31, 385–391.

Ertel, E.A., Campbell, K.P., Harpold, M.M., Hofmann, F., Mori, Y., Perez-Reyes, E., Schwartz, A., Snutch, T.P., Tanabe, T., Birnbaumer, L., Tsien, R.W., Catterall, W.A., 2000. Nomenclature of voltage-gated calcium channels. Neuron 25, 533–535.

Foncea, R., Andersson, M., Ketterman, A., Blakesley, V., Sapag-Hagar, M., Sugden, P.H., LeRoith, D., Lavandero, S., 1997. Insulin-like growth factor-I rapidly activates multiple signal transduction pathways in cultured rat cardiac myocytes. J. Biol. Chem. 272, 19115–19124.

Hishikawa, K., Luscher, T.F., 1998. Felodipine inhibits free-radical production by cytokines and glucose in human smooth muscle cells. Hypertension 32, 1011–1015.

Jiang, Y., Lee, A., Chen, J., Ruta, V., Cadene, M., Chait, B.T., MacKinnon, R., 2003. X-ray structure of a voltage-dependent K+ channel. Nature 423, 33–41.

Kourie, J.I., 1997. A redox O_2 sensor modulates the SR Ca^{2+} countercurrent through voltage- and Ca^{2+}-dependent Cl-channels. Am. J. Physiol. 272, C324–C332.

Kourie, J.I., 1998. Interaction of reactive oxygen species with ion transport mechanisms. Am. J. Physiol. 275, C1–C24.

Krzeminski, T.F., Mitrega, K., Varghese, B., Hudziak, D., Porc, M., Kedzia, A., Sielanczyk, A. W., Jablecka, A., Jasinski, M., 2011. Cardioprotective effects of an active *meta*bolite of furnidipine in 2 models of isolated heart and on in vivo ischemia-induced and reperfusion-induced arrhythmias in rats. J. Cardiovasc. Pharmacol. 57, 183–193.

Lopez-Alarcon, C., Navarrete, P., Camargo, C., Squella, J.A., Nunez-Vergara, L.J., 2003. Reactivity of 1,4-dihydropyridines toward alkyl, alkylperoxyl radicals, and ABTS radical cation. Chem. Res. Toxicol. 16, 208–215.

Mashimo, K., Ohno, Y., 2006. Ethanol hyperpolarizes mitochondrial membrane potential and increases mitochondrial fraction in cultured mouse myocardial cells. Arch. Toxicol. 80, 421–428.

Mason, R.P., Trumbore, M.W., 1996. Differential membrane interactions of calcium channel blockers. Implications for antioxidant activity. Biochem. Pharmacol. 51, 653–660.

Mason, R.P., Mak, I.T., Trumbore, M.W., Mason, P.E., 1999a. Antioxidant properties of calcium antagonists related to membrane biophysical interactions. Am. J. Cardiol. 84, 16L–22L.

Mason, R.P., Walter, M.F., Trumbore, M.W., Olmstead Jr., E.G., Mason, P.E., 1999b. Membrane antioxidant effects of the charged dihydropyridine calcium antagonist amlodipine. J. Mol. Cell. Cardiol. 31, 275–281.

Millard, R.W., Grupp, G., Grupp, I.L., DiSalvo, J., DePover, A., Schwartz, A., 1983. Chronotropic, inotropic, and vasodilator actions of diltiazem, nifedipine, and verapamil. A comparative study of physiological responses and membrane receptor activity. Circ. Res. 52, I29–I39.

Morris, G.M., Goodsell, D.S., Halliday, R.S., Huey, R., Hart, W.E., Belew, R.K., Olson, A.J., 1998. Automated docking using a lamarckian genetic algorithm and a empirical binding free energy function. J. Comput. Chem. 19, 1639–1662.

Nakamura, K., Miura, D., Kusano, K.F., Fujimoto, Y., Sumita-Yoshikawa, W., Fuke, S., Nishii, N., Nagase, S., Hata, Y., Morita, H., Matsubara, H., Ohe, T., Ito, H., 2009. 4-Hydroxy-2-nonenal induces calcium overload via the generation of reactive oxygen species in isolated rat cardiac myocytes. J. Card. Fail. 15, 709–716.

Nunez-Vergara, L.J., Lopez-Alarcon, C., Navarrete-Encina, P.A., Atria, A.M., Camargo, C., Squella, J.A., 2003. Electrochemical and EPR characterization of 1,4-dihydropyridines. Reactivity towards alkyl radicals. Free Radic. Res. 37, 109–120.

Nunez-Vergara, L.J., Salazar, R., Camargo, C., Carbajo, J., Conde, B., Navarrete-Encina, P.A., Squella, J.A., 2007. Oxidation of C4-hydroxyphenyl 1,4-dihydropyridines in dimethylsulfoxide and its reactivity towards alkylperoxyl radicals in aqueous medium. Bioorg. Med. Chem. 15, 4318–4326.

Pearl, J.M., Plank, D.M., McLean, K.M., Wagner, C.J., Duffy, J.Y., 2011. Glucocorticoids improve calcium cycling in cardiac myocytes after cardiopulmonary bypass. J. Surg. Res. 167, 279–286.

Peterson, B.Z., Catterall, W.A., 2006. Allosteric interactions required for high-affinity binding of dihydropyridine antagonists to Ca(V)1.1 channels are modulated by calcium in the pore. Mol. Pharmacol. 70, 667–675.

Pravdic, D., Vladic, N., Bosnjak, Z.J., 2009. Intracellular Ca^{2+} modulation during short exposure to ischemia-mimetic factors in isolated rat ventricular myocytes. Coll. Antropol. 33 (Suppl. 2), 121–126.

Salazar, R., Navarrete-Encina, P.A., Camargo, C., Squella, J.A., Núñez-Vergara, L.J., 2008. Electrochemical oxidation of C4-vanillin- and C4-isovanillin-1,4-dihydropyridines in aprotic medium: reactivity towards free radicals. J. Electroanal. Chem. 622, 29–36.

Scholz, H., 1997. Pharmacological aspects of calcium channel blockers. Cardiovasc. Drugs Ther 10 (Suppl. 3), 869–872.

Schramm, M., Thomas, G., Towart, R., Franckowiak, G., 1983. Activation of calcium channels by novel 1,4-dihydropyridines. A new mechanism for positive inotropics or smooth muscle stimulants. Arzneimittelforschung 33, 1268–1272.

Snabaitis, A.K., Muntendorf, A., Wieland, T., Avkiran, M., 2005. Regulation of the extracellular signal-regulated kinase pathway in adult myocardium: differential roles of G(q/11), Gi and G(12/13) proteins in signalling by alpha1-adrenergic, endothelin-1 and thrombin-sensitive protease-activated receptors. Cell. Signal. 17, 655–664.

Sugawara, H., Tobise, K., Kikuchi, K., 1996. Antioxidant effects of calcium antagonists on rat myocardial membrane lipid peroxidation. Hypertens. Res. 19, 223–228.

Tikhonov, D.B., Zhorov, B.S., 2005. Modeling P-loops domain of sodium channel: homology with potassium channels and interaction with ligands. Biophys. J. 88, 184–197.

Tikhonov, D.B., Zhorov, B.S., 2008. Molecular modeling of benzothiazepine binding in the L-type calcium channel. J. Biol. Chem. 283, 17594–17604.

Tikhonov, D.B., Zhorov, B.S., 2009. Structural model for dihydropyridine binding to L-type calcium channels. J. Biol. Chem. 284, 19006–19017.

Triggle, D.J., 2007. Calcium channel antagonists: clinical uses—past, present and future. Biochem. Pharmacol. 74, 1–9.

Triggle, A.M., Shefter, E., Triggle, D.J., 1980. Crystal structures of calcium channel antagonists: 2,6-dimethyl-3,5-dicarbomethoxy-4-[2-nitro-, 3-cyano-, 4-(dimethylamino)-, and 2,3,4,5,6-pentafluorophenyl]-1,4-dihydropyridine. J. Med. Chem. 23, 1442–1445.

Walsh, C.P., Davies, A., Nieto-Rostro, M., Dolphin, A.C., Kitmitto, A., 2009. Labelling of the 3D structure of the cardiac L-type voltage-gated calcium channel. Channels 3, 387–392.

Waring, P., 2005. Redox active calcium ion channels and cell death. Arch. Biochem. Biophys. 434, 33–42.

Xu, Y.J., Gopalakrishnan, V., 1991. Vasopressin increases cytosolic free [Ca^{2+}] in the neonatal rat cardiomyocyte. Evidence for V1 subtype receptors. Circ. Res. 69, 239–245.